X-763-71-125

PREPRINT

NASA TM X- 65534

MATHEMATICAL ANALYSIS OF A VUILLEUMIER REFRIGERATOR

ALLAN SHERMAN

MARCH 1971

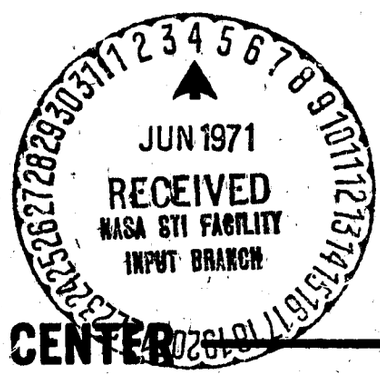

GODDARD SPACE FLIGHT CENTER
GREENBELT, MARYLAND

X-763-71-125

MATHEMATICAL ANALYSIS OF A VUILLEUMIER REFRIGERATOR

Allan Sherman

March 1971

Goddard Space Flight Center
Greenbelt, Maryland

ABSTRACT

A comprehensive analysis of the Vuilleumier refrigerator was conducted. This analysis includes the effects of non-isothermal gas heat addition and rejection, hot and cold regenerator inefficiencies, conduction losses, and gas leakage losses. A computer program was written which solves the equations resulting from the analysis. The program calculates internal pressures, temperatures, and gas flow rates as functions of refrigerator crank angle, as well as overall refrigerator cooling load and power input. Comparisons between the program results and available data show good agreement, with a marked improvement over the predictions of the ideal model.

PRECEDING PAGE BLANK NOT FILMED

CONTENTS

MATHEMATICAL ANALYSIS OF A VUILLEUMIER REFRIGERATOR

by
Allan Sherman
Goddard Space Flight Center

I. INTRODUCTION

The Vuilleumier (VM) refrigeration concept was patented in the United States in 1918. Apparently, because of its low efficiency and cooling load when compared with other low-temperature refrigerators, its development was not pursued. However, there has recently been much interest in the development of a VM cryogenic refrigerator for spacecraft application, because a refrigerator of this type has the potential advantages of long lifetime operation, compactness, and low weight.

Figure 1 shows a possible design for a cryogenic VM refrigerator for spacecraft application. The refrigerator consists of a hot cylinder to which heat is transferred from a heat source, a cold cylinder to which heat is transferred from the load (e.g., spacecraft sensors), and a sump from which heat is rejected to the ambient (e.g., spacecraft radiator). The gas (e.g., helium) is at a different temperature in each of these three sections ($T_H > T_A > T_C$)*, and continuously flows through the regenerators into each section, due to the motion of the displacers as the crankshaft rotates. The gas temperature differences among the sections are maintained by the displacers, which are thermal barriers; the regenerators, which heat or cool the flowing gases to the appropriate temperatures; and the heat transfer to or from each section.

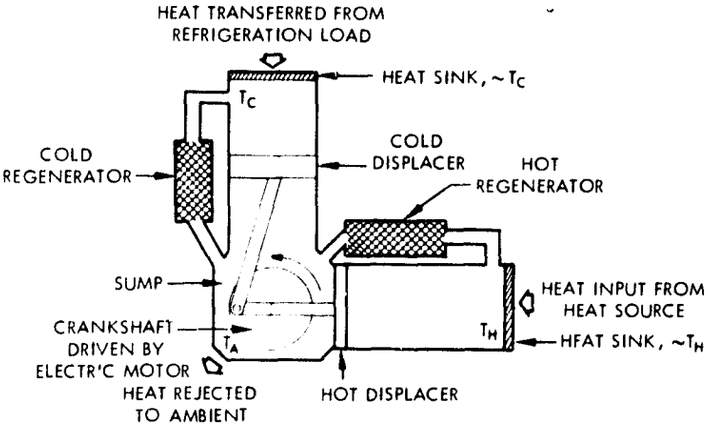

Figure 1. VM Refrigerator

*For discussion purposes, we assume that the individual cylinder gas temperatures are constant. Actually, as will be pointed out later, the cylinder gas temperatures fluctuate during the cycle.

With reference to Figure 1, the reasons for the advantages of the VM refrigerator for spacecraft application are:

(1) Compactness and Low Weight: By its very design the VM refrigerator is essentially a one-component system (i.e., the compressor and expander are in one housing), and, for the low required cooling loads of spacecraft sensors, is of relatively low weight. Furthermore, as will be discussed, the power required to drive the VM is very low, and thus a large motor is not required. However, a heat source (e.g., a radiosotope type) is needed.

(2) Long Lifetime Operation: The pressure differences among the three sections of the VM refrigerator are very small. Hence, piston pressure seals are not required (as contrasted to other possible refrigeration concepts such as the Stirling cycle), and, in fact, a feasible seal design might be just a clearance between the displacers and cylinder walls. Thus failure by pressure seal wear could be eliminated and lower rolling bearing forces could be attained.

II. BASIC VM OPERATION

The VM cooler (Figure 1) is essentially a heat engine driving a refrigerator. Thus the input energy to the device is supplied as heat, which minimizes the required drive-motor size, and allows the direct use of a long lifetime heat source such as a radioactive isotope. The displacers move the gas from one cylinder of the refrigerator to the other, but do not directly compress or expand the gas.

The steady state operation of the VM refrigeration cycle will now be explained. Reference will be made to Figure 2 (a schematic of four crank positions encountered during operation, and Figure 3 (the pressure-volume diagrams for the cold cylinder, hot cylinder, and total gas volume for the VM cycle). In this explanation we assume that the pressure drop across the regenerators is zero, and thus for the design depicted the pressures in the three sections are always equal. (In the actual case, the regenerator pressure drops are comparatively small.) Furthermore, we note that the shapes of the pressure-volume diagrams in Figure 3 are close to those resulting from the crank type of design shown in Figure 1. One could conceive of a displacer movement scheme which would result in more idealized VM performance (i.e., higher thermal efficiency), but the required mechanism would not be practical for long time spacecraft use. Finally, it should be noted that the following is a simplified view of the operation of the VM engine, in that only the predominant processes for a given crank position are pointed out. The actual operation of the refrigerator is much more complicated, as the subsequent mathematical analysis will show.

We begin with the crank in the South position (Figure 2). At this point the cold displacer is at its maximum displacement position, and the hot displacer is only at its half-maximum position.

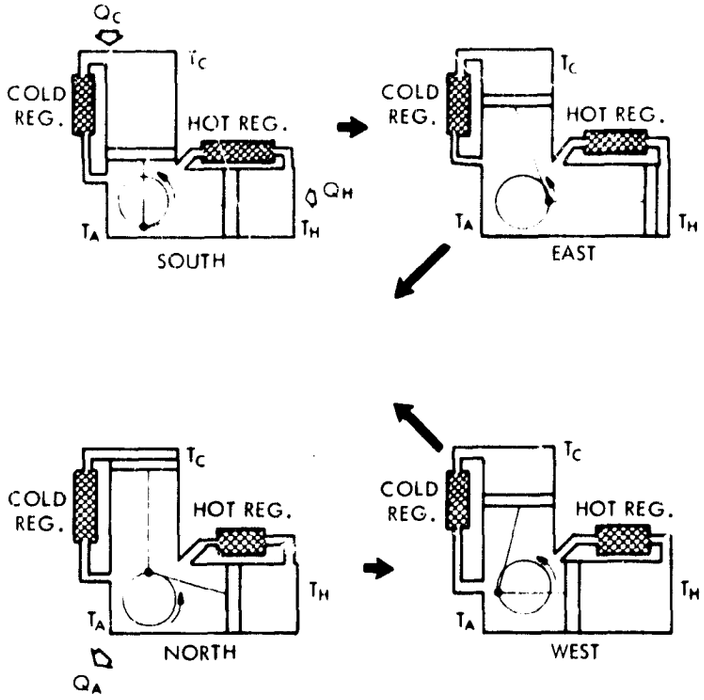

Figure 2. VM Refrigerator Operation

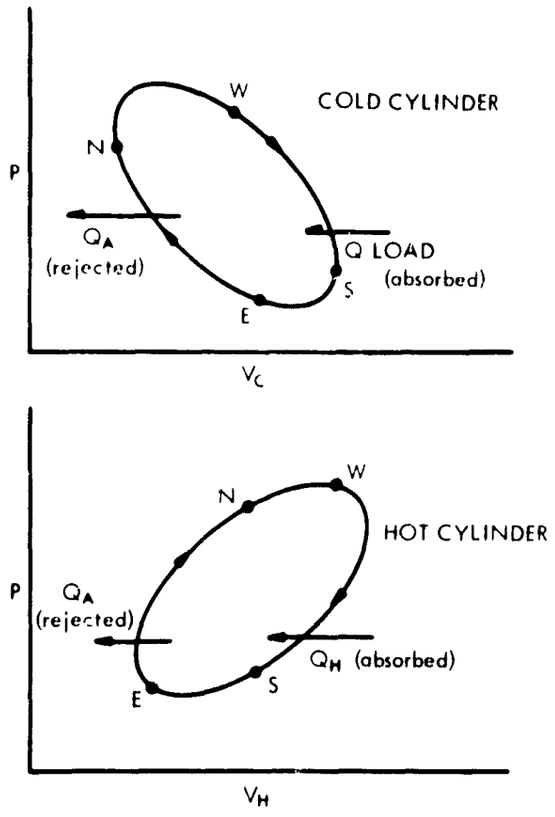

Figure 3. Pressure-Volume Diagrams for the VM Cycle

The mean gas temperature in the VM refrigerator is relatively low, and consequently the gas pressure is low. This is shown in the hot cylinder and cold cylinder P-V diagrams in Figure 3. Since this low pressure is the result of the West-South expansion process (as will be shown), heat is absorbed from the refrigeration load and heat source.

As the crank turns to the East position, both the hot and cold cylinder volumes decrease. Part of the cold gas is forced through the cold regenerator, which is at some mean temperature, $\overline{T}_{CRG}$ * ($T_C < \overline{T}_{CRG} < T_A$), where it is heated to nearly T_A before entering the ambient section. Similarly, most of the hot cylinder gas is forced through the hot regenerator which is at some mean temperature, $\overline{T}_{HRG}$ ($T_A < \overline{T}_{HRG} < T_H$), where it is cooled to nearly T_A before entering the ambient section. Heat, which is to be used later in the cycle, is thus stored in the hot regenerator. Finally, since both the hot cylinder volume and cold cylinder volume have decreased, the mean gas temperature, and consequently the gas pressure, change very little during this process. Nevertheless,

*The temperature along the length of the hot and cold regenerator matrices varies from a temperature somewhat less than the gas temperature at the hot end to somewhat greater than the gas temperature at the cold end.

some gas expansion (caused by the small pressure drop that does occur), with the resulting heat absorption from the load, does take place.

As the crank moves from East to North, the hot cylinder volume increases and the cold cylinder volume decreases. The cold gas which is forced through the cold regenerator is heated to nearly T_A, while part of the ambient gas flows through the hot regenerator, is heated (from stored energy) to nearly T_H, and enters the hot cylinder. The net effect of the hot cylinder volumetric increase and the cold cylinder decrease is an increase in the mean gas temperature and gas pressure. Hence, this process is one of gas compression, and for the temperatures to remain constant, heat must be rejected. Therefore, heat is rejected at the ambient section.

As the crank turns from North to West, the volumes of both the hot cylinder and cold cylinder increase. Part of the ambient gas moves through the cold regenerator, releases heat to it, and enters the cold volume at nearly T_C. On the hot side, part of the ambient gas moves through the hot regenerator, absorbs heat, and enters the hot volume at nearly T_C. Since both the cold volume and hot volume increase, the system pressure does not greatly change. Nevertheless, there is some compression with a corresponding heat rejection at the ambient section.

The crank now turns from West to South, decreasing the hot cylinder volume while increasing the cold cylinder volume. Part of the hot cylinder gas is forced through the hot regenerator where it is cooled to nearly T_A, while part of the ambient gas is forced through the cold regenerator where it is cooled to nearly T_C. The mean gas temperature, and consequently the gas pressure, decreases, resulting in gas expansion. This causes heat absorption at the cold and hot ends.

III. ISOTHERMAL IDEAL MODEL

The isothermal ideal mathematical model assumes isothermal expansion and compression of the gas in each cylinder, 100% thermally efficient regenerators, zero pressure drop across the regenerators, no displacer sliding friction, and no bearing friction. From the first law of thermodynamics for the hot cylinder over one cycle,

$$\oint dQ = \oint dU + \oint p\,dV - \oint h_1\,dm_1. \tag{1}$$

For a regenerator with 100% thermal efficiency,

$$\oint h_1\,dm_1 = 0, \tag{2}$$

and since the gas in the cylinder returns to its initial state after one cycle,

$$\oint dU = 0. \tag{3}$$

Thus, over one cycle,

$$Q_H = \oint p\, dV_H. \tag{4}$$

Similarly,

$$Q_C = \oint p\, dV_C. \tag{5}$$

Now, from the equation of state and the conservation of mass, we have at any time during the cycle

$$p = M_0 R \Big/ \left[\frac{V_H}{T_H} + \frac{V_C}{T_C} + \frac{V_A}{T_A} + \frac{V_{HP}}{T_{HRG}} + \frac{V_{CR}}{T_{CRG}}\right]. \tag{6}$$

The volumes V_C, V_A, V_H can be computed as functions of the crank angle. V_{HR}, V_{CR}, T_H, T_C, T_A, T_{CR}, and T_{HR} are constants. Hence, Equations (4) and (5) can be expressed in terms of the variable θ, and integrated from $\theta = 0$ to $\theta = 2\pi$ (one cycle). Explicit expressions for the cooling load $\dot{Q}_C$ and hot cylinder power requirement $\dot{Q}_H$ can then be obtained (Reference 1).

The inadequacy of this model becomes all too obvious when we compare experimental results with theoretical predictions. Typically, the above analysis may predict a cooling load of 10 watts and a hot cylinder heat input of 50 watts when the actual values are about 2 watts and 180 watts, respectively. These discrepancies prompted investigators to correct the ideal model by estimating various losses, such as regenerator inefficiency, for the whole cycle, and then adding these losses to the ideal model results. This process of uncoupling the losses from the engine performance resulted in only limited success, with little confidence in the predictions because of a lack of theoretical justification for such a process.

The analysis presented in this report was initiated with the goal of providing a program for more confidently predicting VM refrigerator performance, and more accurately weighing design trade-offs. An attempt was made to include as many losses as possible without the uncoupling assumptions. In order to do this, all processes were expressed in the form of partial differential equations, and the resulting rather complicated system of equations was solved via a computer program.

IV. ANALYSIS

A. General Configuration

Figure 4 shows a schematic of a VM refrigerator with the significant variables employed for the analysis. It should be emphasized that this figure is only a schematic and that the analysis is not limited to the particular geometry shown. For example, the regenerators could be located within the refrigerator without affecting the subsequent equations. Furthermore, the directions of the arrows in the figure are arbitrary.

The heat exchange area for each cylinder is subdivided into the cylinder wall and heat exchanger entrance regions. In this way, flexibility is obtained in matching the actual VM geometry to that of the mathematical model.

The walls of the cylinder and heat exchanger are assumed to be at a constant temperature (T_{HW}, T_{AW}, T_{CW}) for each cylinder section. This means that we are assuming the cylinder walls and end caps to be infinite heat sinks (or sources) relative to the fluctuating gas temperatures. This is indeed close to the actual case for most VM refrigerator designs.

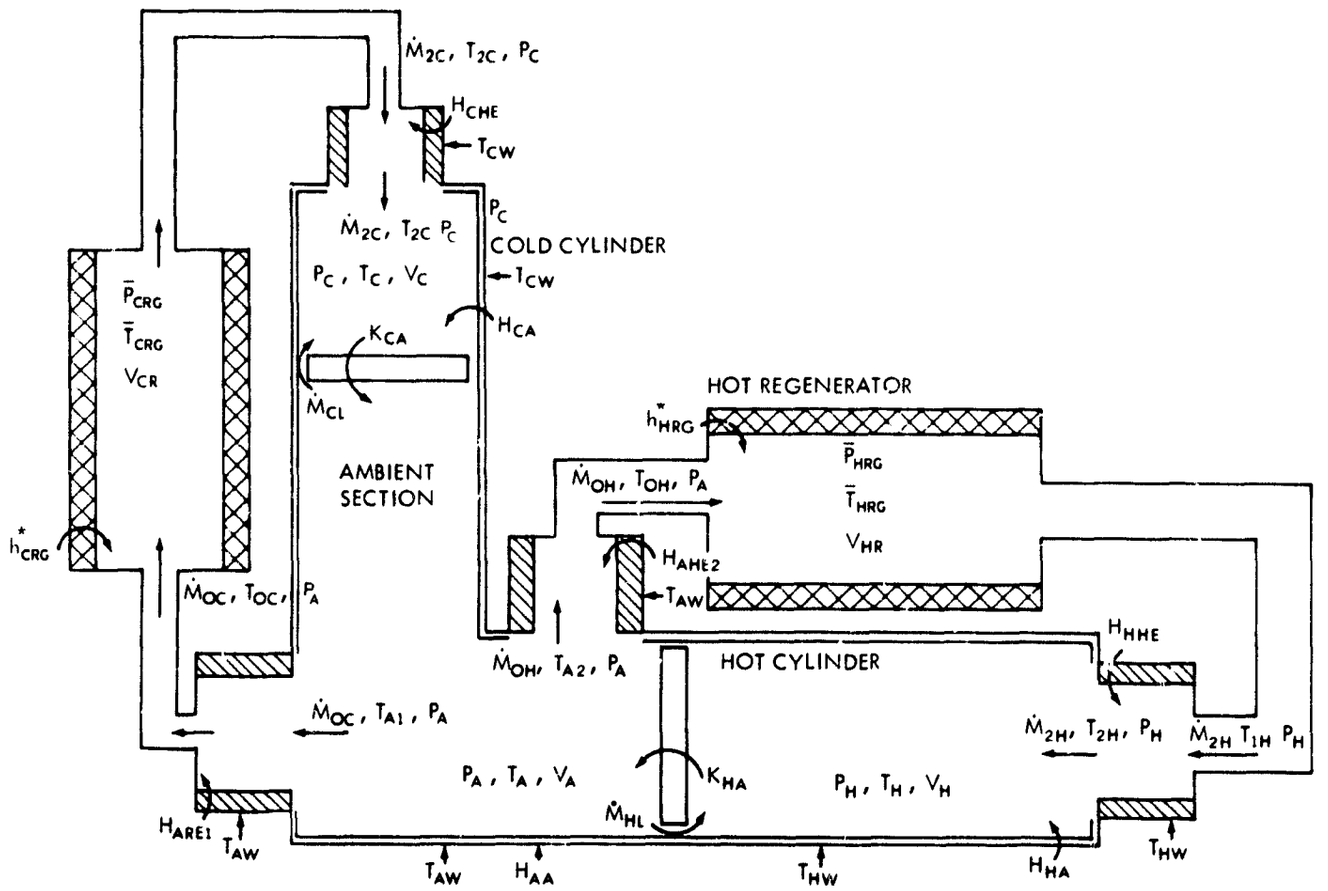

Figure 4. VM Refrigerator Schematic

B. Geometric Equations

A schematic of the geometric arrangement of the VM refrigerator with dimensions labeled is shown in Figure 5. The crank angle θ is measured from the axis of the cold cylinder and thus at $\theta = 0$ the cold displacer is at top dead center.

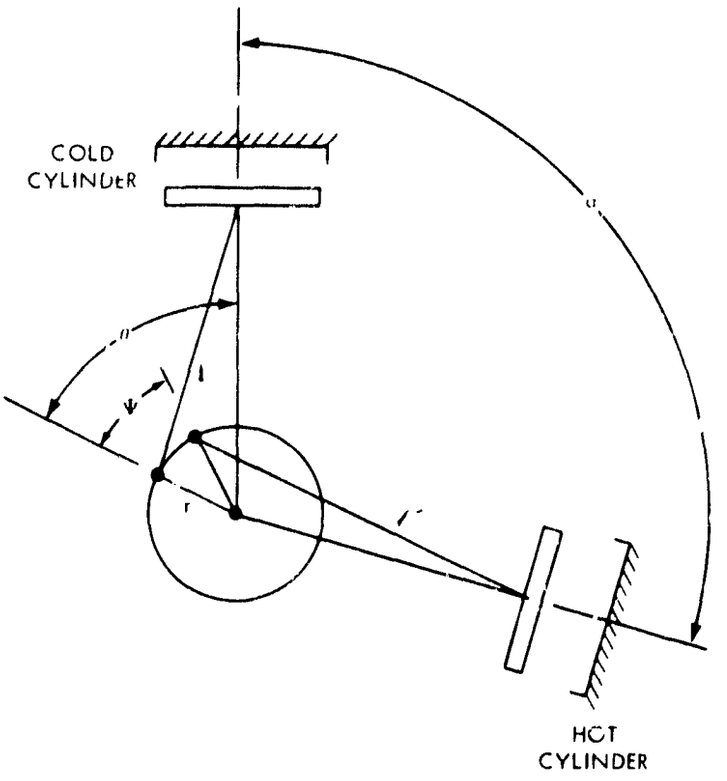

Figure 5. Geometric Arrangement of the VM Refrigerator

From simple geometric considerations, then, it is shown in Appendix A that

$$V_C = \frac{V_{CMAXD}}{2}\left[\frac{\ell}{r}\left[1 - \cos\left(\sin^{-1}\left(\frac{r}{\ell}\sin\theta\right)\right)\right] + (1 - \cos\theta)\right] + V_{CD}, \tag{7}$$

$$V_H = \frac{V_{HMAXD}}{2}\left\{\frac{\ell'}{r}\left[1 - \cos\left[\sin^{-1}\left(\frac{r}{\ell'}\sin(\alpha + \theta - \Psi)\right)\right]\right] + 1 - \cos(\alpha + \theta - \Psi)\right\} + V_{HD}, \tag{8}$$

and

$$V_A = V_{HD} + V_{CD} + V_{AD} + V_{CMAXD} + V_{HMAXD} - V_C - V_H. \tag{9}$$

Differentiating Equations (7) through (9) with respect to time, we have

$$\dot{V}_C = \frac{V_{CMAXD}}{2}\left[\left(\frac{r}{\ell}\sin\theta\right)\frac{\omega\cos\theta}{\sqrt{1 - \left(\frac{r}{\ell}\sin\theta\right)^2}} + \omega\sin\theta\right], \tag{10}$$

$$\dot{V}_H = \frac{V_{HMAXD}}{2}\left[\left(\frac{r}{\ell'}\sin(\theta + \alpha - \Psi)\right)\frac{\omega\cos(\alpha + \theta - \Psi)}{\sqrt{1 - \left(\frac{r}{\ell'}\sin(\alpha + \theta - \Psi)\right)^2}} + \omega\sin(\alpha + \theta - \Psi)\right], \tag{11}$$

and

$$\dot{V}_A = -\dot{V}_C - \dot{V}_H. \tag{12}$$

These geometric equations describe the cylinder volumes and time rates of change of the volumes as functions of crank position, crank assembly dimensions, and rotational speed, and are used later in the analysis.

C. Cylinder Equations

Referring to Figure 4 for the hot cylinder, we have from the First Law of Thermodynamics (neglecting gas kinetic energy terms),

$$d Q = d U + p_H d V_H - h_1 d m_1 - h_2 d m_2 \tag{13}$$

where, from the perfect gas law,

$$p_H = \frac{M_H}{V_H} R T_H, \tag{14}$$

and we take

$$h_1 d m_1 = C_p T_{2H} \dot{M}_{2H} d t, \tag{15}$$

$$h_2 d m_2 = C_p T_H \dot{M}_{HL} d t. \tag{16}$$

Note that in Equation (16) we are assuming that the leakage gas around the displacer enters and leaves the hot cylinder at T_H. This assumption is exact when the gas leaks from the hot cylinder to the ambient cylinder; it is a reasonable simplifying approximation when the gas flows from the ambient cylinder to the hot section.

Now

$$d Q = [H_{HA} (T_W - T_H) + K_{HA} (T_A - T_H)] d t \tag{17}$$

and

$$d U = d (M_H C_V T_H) = M_H C_V d T_H + C_V T_H d M_H. \tag{18}$$

Combining and simplifying Equations (13) through (18) and transforming the independent variable via

$$d \theta = \omega d t \tag{19}$$

yields

$$\frac{d T_H}{d\theta} = \frac{1}{\omega}\left[\frac{H_{HA}(T_{HW} - T_H)}{M_H C_V} + \frac{K_{HA}(T_A - T_H)}{M_H C_V} - \frac{T_H \frac{d M_H}{d t}}{M_H} - \frac{(\gamma - 1) T_H \dot{V}_H}{V_H} + \frac{\gamma T_{2H} \dot{M}_{2H}}{M_H} - \frac{\gamma T_H \dot{M}_{HL}}{M_H}\right], \tag{20}$$

where

$$\frac{d M_H}{d t} = \dot{M}_{2H} + \dot{M}_{HL}. \tag{21}$$

From a similar analysis for the cold and ambient sections, we have

$$\frac{d T_C}{d\theta} = \frac{1}{\omega}\left[\frac{H_{CA}(T_{CW} - T_C)}{M_C C_V} + \frac{K_{CA}(T_A - T_C)}{M_C C_V} - \frac{T_C \frac{d M_C}{d t}}{M_C} - \frac{(\gamma - 1) T_C \dot{V}_C}{V_C} + \frac{\gamma T_{2C} \dot{M}_{2C}}{M_C} + \frac{\gamma T_C \dot{M}_{CL}}{M_C}\right], \tag{22}$$

$$\frac{d T_A}{d\theta} = \frac{1}{\omega}\left[\frac{H_{AA}(T_{AW} - T_A)}{M_A C_V} + \frac{K_{HA}(T_H - T_C)}{M_A C_V} + \frac{K_{CA}(T_A - T_C)}{M_A C_V} - \frac{T_A \frac{d M_A}{d t}}{M_A} - \frac{(\gamma - 1) T_A \dot{V}_A}{V_A}\right.$$
$$\left. + \frac{\gamma \dot{M}_{OC} T_{A1}}{M_A} + \frac{\gamma \dot{M}_{OH} T_{A2}}{M_A} - \frac{\gamma T_A \dot{M}_{CL}}{M_A} - \frac{\gamma T_A \dot{M}_{HL}}{M_A}\right], \tag{23}$$

where

$$\frac{d M_C}{d t} = \dot{M}_{2C} + \dot{M}_{CL}, \tag{24}$$

and

$$\frac{d M_A}{d t} = \dot{M}_{OC} + \dot{M}_{OH} - \dot{M}_{HL} - \dot{M}_{CL}. \tag{25}$$

D. Heat Exchange Sections

For the heat exchange sections, we assume the total volume and hence the gas storage to be negligible. Thus we use the usual steady state heat exchanger equations for a constant wall temperature. We can then say

$$T_{HOUT} = \left(1 - e^{-\frac{h^{**}}{W C_p}}\right)(T_W - T_{HIN}) + T_{HIN}, \tag{26}$$

where the variables are assigned as shown in Table 1. We also assume that the pressure drops across the heat exchange sections are negligible compared to the regenerator gas pressure drops.

Table 1

Variables Used in the Heat Exchanger Equation (26)

Cold Heat Exchanger		Hot Heat Exchanger	
$P_C \geq \bar{P}_{CRG}$	$P_C < \bar{P}_{CRG}$	$P_H < \bar{P}_{HRG}$	$P_H \geq \bar{P}_{HRG}$
$h^{**} = H_{CHE}$	$h^{**} = H_{CHE}$	$h^{**} = H_{HHE}$	$h^{**} = H_{HHE}$
$T_{HIN} = T_{2C}$	$T_{HIN} = T_{1C}$	$T_{HIN} = T_{1H}$	$T_{HIN} = T_{2H}$
$T_{HOUT} = T_{1C}$	$T_{HOUT} = T_{2C}$	$T_{HOUT} = T_{2H}$	$T_{HOUT} = T_{1H}$
$W = \dot{M}_{1C}$	$W = \dot{M}_{2C}$	$W = \dot{M}_{2H}$	$W = \dot{M}_{2H}$
$T_W = T_{CW}$	$T_W = T_{CW}$	$T_W = T_{HW}$	$T_W = T_{HW}$
Ambient Heat Exchanger Number 1		Ambient Heat Exchanger Number 2	
$P_A < \bar{P}_{CRG}$	$P_A \geq \bar{P}_{CRG}$	$P_A < \bar{P}_{HRG}$	$P_A \geq \bar{P}_{HRG}$
$h^{**} = H_{AHE1}$	$h^{**} = H_{AHE1}$	$h^{**} = H_{AHE2}$	$h^{**} = H_{AHE2}$
$T_{HIN} = T_{OC}$	$T_{HIN} = T_{A1}$	$T_{HIN} = T_{OH}$	$T_{HIN} = T_{A2}$
$T_{HOUT} = T_{A1}$	$T_{HOUT} = T_{OC}$	$T_{HOUT} = T_{A2}$	$T_{HOUT} = T_{OH}$
$W = \dot{M}_{OC}$	$W = \dot{M}_{OC}$	$W = \dot{M}_{OH}$	$W = \dot{M}_{OH}$
$T_W = T_{AW}$	$T_W = T_{AW}$	$T_W = T_{AW}$	$T_W = T_{AW}$

E. Regenerators (Hot or Cold)

For the purposes of this analysis, we assume that the regenerators are of uniform geometry and material along their lengths, and describable by a free-flow area A_R, and a wetted perimeter P*. In addition, we are assuming that both the gas in each regenerator and the material of the regenerators have constant specific heat.

Assuming one-dimensional flow, the energy equation (dropping the gas kinetic energy term) for an infinitesimal slab of gas, perpendicular to the regenerator axis, and of mass dm is

$$\frac{dQ}{dt} = \frac{\partial h}{\partial x} dx + \frac{\partial U}{\partial t} \tag{27}$$

Now,

$$\frac{\partial h}{\partial x} = \dot{m} C_p \frac{\partial T_g}{\partial x} + C_p T_g \frac{\partial \dot{m}}{\partial x} \tag{28}$$

and

$$\frac{\partial U}{\partial t} = (d m)\, C_V \frac{\partial T_g}{\partial t} + T_g\, C_V \frac{\partial (d m)}{\partial t}, \tag{29}$$

where

$$d m = \rho A_R\, d x. \tag{30}$$

In addition we may write

$$-\frac{\partial \dot{m}}{\partial x} = A_R \frac{\partial \rho}{\partial t} \tag{31}$$

and

$$\frac{d Q}{d t} = h^* P^* (T_R - T_g)\, d x. \tag{32}$$

Combining and simplifying Equations (27) through (32), while changing the independent variable from t to θ, yields

$$\frac{\partial T_g}{\partial \theta} = \frac{1}{\omega} \frac{\left[J (\gamma - 1)\, T_g\, h^* P^* (T_R - T_g) - \dot{m} C_p (\gamma - 1)\, T_g\, J \left(\frac{\partial T_g}{\partial x}\right) - R\, T_g^2 (\gamma - 1) \frac{\partial \dot{m}}{\partial x} \right]}{P_g A_R} \tag{33}$$

Now, an energy balance in the corresponding metal regenerator slab, ignoring axial conduction, is

$$\frac{C_{PR} M_R}{L_{RG}} \frac{\partial T_R}{\partial \theta} = \frac{1}{\omega} h^* (T_g - T_R), \tag{34}$$

from which

$$\frac{\partial T_R}{\partial \theta} = \frac{1}{\omega} \left[\frac{h^*}{(M_R / L_{RG})\, C_{PR}} (T_g - T_R) \right]. \tag{35}$$

The convective heat transfer coefficient h in Equations (32) - (34) is assumed to be of the form

$$h^* = D \dot{m}^E, \tag{36}$$

where D and E are obtained from experimental data (e.g., Reference 3).

In order to solve Equations (32) and (35), and to calculate the corresponding mass flow rates, a "lumped" type of approximation similar to that used in Reference 2 is employed. For the purpose

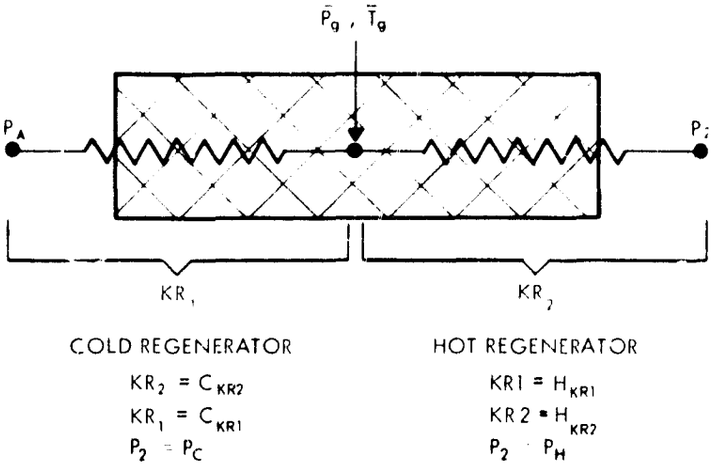

Figure 6. Illustrated of Lumped Flow Resistance Approximation

of this approximation the gas in each regenerator is considered to be at an average temperature $\bar{T}_g$ given by

$$\bar{T}_g = \frac{1}{L_{RG}} \int_0^{L_{RG}} T_g(x)\, dx, \tag{37}$$

and an average pressure given by

$$\bar{P}_g = \frac{M_g}{V_{RG}} R \bar{T}_g. \tag{38}$$

The flow resistance for each regenerator half is then lumped into a flow resistance coefficient. The assumption is illustrated in Figure 6 which shows the three modes among which we wish to calculate the gas mass flow rate. The appropriate flow resistance coefficients and pressures are labeled.

The mass flow rate into and out of either end of the regenerator is then calculated from

$$\frac{\partial M_1}{\partial \theta} = \pm \frac{1}{\omega} \sqrt{\frac{|P_A - \bar{P}_g|\, \bar{P}_g / R \bar{T}_g}{K R_1}} \quad \left(\begin{array}{c}\text{for the ambient end}\\ \text{of the hot or}\\ \text{cold regenerator}\end{array}\right) \tag{39}$$

$$\frac{\partial M_2}{\partial \theta} = \pm \frac{1}{\omega} \sqrt{\frac{|P_2 - \bar{P}_g|\, \bar{P}_g / R \bar{T}_g}{K R_2}} \left(\begin{array}{c}\text{for the hot or}\\ \text{cold end of the}\\ \text{regenerators}\end{array}\right), \tag{40}$$

where the constants KR_1, KR_2 are calculated from experimental data (e.g., as contained in Reference 3) for the particular regenerator, and the sign in front of the radical is determined from an appropriate sign convention.*

Now, in order to facilitate solving Equations (33) and (35) we make the following three approximations in these two equations:

*Details of the sign convention for Equations (39) and (40) are given in Reference 4. The signs in front of these equations are of no significance in this discussion.

$$\frac{\dot{m}}{x} \simeq - \left| \frac{\dot{M}_1 + \dot{M}_2}{L_{RG}} \right|, \tag{41}$$

$$\dot{M} \simeq \left| \frac{\dot{M}_1 - \dot{M}_2}{2} \right|, \tag{42}$$

and

$$P_g \simeq \bar{P}_g, \tag{43}$$

where again the signs in front of the terms are from a compatable sign convention. In effect, Equations (41) and (42) represent an average value for the regeneration mass flow rate and mass flow rate gradient, respectively.

F. Internal Mass Flow Rates

With the lumping of the regenerators' flow resistance, the mass flow rates into and out of each cylinder can be calculated. Again, we assume the regenerator gases to be at an average pressure and temperature given by Equations (37) and (38), and we calculate the flow rate to a point at this temperature and pressure. Experimental data are used to obtain the flow resistance coefficient for each half of the regenerator.

The internal mass flow rates can then be calculated by the equations

$$\dot{M}_{2C} = \pm \sqrt{\frac{|P_C - \bar{P}_{CRG}| \, \bar{P}_{CRG} / R \, \bar{T}_{CRG}}{C_{KR2}}}, \tag{44}$$

$$\dot{M}_{OC} = \pm \sqrt{\frac{|P_A - \bar{P}_{CRG}| \, \bar{P}_{CRG} / R \, \bar{T}_{CRG}}{C_{KR1}}}, \tag{45}$$

$$\dot{M}_{OH} = \pm \sqrt{\frac{|P_A - \bar{P}_{HRG}| \, \bar{P}_{HRG} / R \, \bar{T}_{HRG}}{H_{KR1}}}, \tag{46}$$

and

$$\dot{M}_{2H} = \pm \sqrt{\frac{|P_H - \bar{P}_{HRG}| \, \bar{P}_{HRG} / \bar{T}_{HRG}}{H_{KR2}}}, \tag{47}$$

G. Leakage and Friction

The gas leakage mass flow rates around the cold and hot displacer are calculated from the laminar Couette flow solution

$$\dot{M}_L = \pi R_D \left[\frac{P_2}{R T_2} + \frac{P_A}{R T_A} \right] \frac{b^3}{12 \mu_g} \frac{(P_A - P_2)}{L_D} \quad (48)$$

The frictional force exerted by the gas on each displacer can then be calculated via the laminar flow solution to the Navier Stokes equations:

$$F = 2 \pi R_D L_D \mu_g \left[\frac{\dot{V}}{A_D} + \frac{b (P_A - P_2)}{2 \mu_g L_D} \right] . \quad (49)$$

The heat transferred to or from the cylinder by the leakage gas is then approximated as

$$\dot{Q}_{CL} = \dot{M}_{CL} C_P (T_C - T_A) \quad (50)$$

and

$$\dot{Q}_{HL} = \dot{M}_{HL} C_P (T_H - T_A), \quad (51)$$

where again we are assuming that the gas is heated or cooled to the gas temperatures in the cylinders to which it is flowing.

H. Heat Transfer, Work, and Performance Computations

The heat transfer rate to the hot cylinder is given by

$$\dot{Q}_H = H_{HA} (T_{HW} - T_H) + \dot{M}_{2H} C_P (T_{2H} - T_{1H}) + K_{HW} (T_{HW} - T_H) + \frac{1}{2} \dot{Q}_{HL}, \quad (52)$$

where the $K_{HW} (T_{HW} - T_{AW})$ term is the heat lost directly from the hot cylinder to the ambient cylinder (i.e., either by radiation or a direct conduction path). One-half of the heat transferred to or from the cylinder wall by the hot-to-ambient cylinder gas leakage is allocated to the hot cylinder.

Similarly, the heat transfer rates to the cold and sump cylinder walls are given by

$$\dot{Q}_C = H_{CA} (T_{CW} - T_C) + \dot{M}_{2C} C_P (T_{2C} - T_{1C})$$

and

$$+ K_{CW} (T_{CW} - T_{AW}) + \frac{1}{2} \dot{Q}_{CL} \quad (53)$$

$$\dot{Q}_A = H_{AA}(T_{AW} - T_A) + K_{CW}(T_{AW} - T_{CW}) + K_{HW}(T_{AW} - T_{HW})$$

$$+ \dot{M}_{OH} C_p (T_{A2} - T_{OH}) + \dot{M}_{OC} C_p (T_{A1} - T_{OC}) + \frac{1}{2}\dot{Q}_{HL} + \frac{1}{2}\dot{Q}_{CL} \quad (54)$$

The average heat transfer rate over one revolution of the crankshaft is obtained by solving Equations (52) - (54) for the total heat transferred to each cylinder over one revolution, and dividing by the cycle period. Hence,

$$\dot{Q}_H = \frac{Q_H}{2\pi/\omega} \quad (55)$$

$$\dot{Q}_C = \frac{Q_C}{2\pi/\omega} \quad (56)$$

and

$$\dot{Q}_A = \frac{Q_A}{2\pi/\omega} \quad (57)$$

The work that must be supplied to each displacer is the sum of the "pdV" work plus the work required to overcome the viscous drag of the gas between the displacers and cylinder walls. The work rate, then, is given by

$$\dot{W}_K = \dot{V}_C (\pm F_C/A_{DC} + P_C) + \dot{V}_H (\pm F_H/A_{DH} + P_H) + P_A \dot{V}_A \quad (58)$$

where F_C and F_H are computed from Equation (49) for the appropriate cylinder, with the sign determined from a compatable sign convention.

The average work rate over one cycle is obtained by solving Equation (58) for the total work and dividing by the cycle period. Hence,

$$\overline{\dot{W}_K} = \frac{W_K}{2\pi/\omega} \quad (59)$$

The coefficient of performance for the VM refrigerator is computed (by definition) from

$$COP = \frac{\dot{Q}_C}{(\dot{Q}_H + |\dot{W}_K|)} \quad (60)$$

where the absolute value sign is required for the work rate term because $\dot{W}_K$ is always negative as a result of the sign convention system employed.

Another measure of performance used here is the percent of Carnot efficiency for a refrigerator operating between T_C and T_A. This is given by

$$CAR \quad \frac{COP}{\left(\frac{T_{CW}}{T_{AW} - T_{CW}}\right)} \tag{61}$$

V. SYSTEM SOLUTION

A computer program (Reference 4) was developed which simultaneously solves the equations developed in sections IV A through IV H. This program employs a combination of finite difference and Runge Kutta numerical techniques to solve the system of equations as functions of crank angle . For most designs, the system consists of several hundred equations, primarily because the regenerators are subdivided axially into slabs (usually about 100 each); thus the energy and momentum equations must be solved for each slab at every . In addition, since the system represents a two-point boundary value problem, an iterative technique on must be employed. Typically, a step size of .004° is used with about 10 iterations and a run time of about 2-1/2 hours.

Because of the large amount of computer time required, the program is not used for general VM refrigeration performance studies, but is primarily employed in the design of a specific Vuilleumier refrigerator.

The input and output variables and constants for the program are listed in Appendix C.

VI. RESULTS

A. Data Correlation

Very little design information or data on Vuilleumier refrigerators has been published. A design is presented, however, in Reference 1; a schematic of this machine, taken from Reference 1, is shown in Figures 7A and 7B. The rather limited available data from testing this refrigerator are used to demonstrate program/test correlation.

The results of the computer program runs for this refrigerator are shown in Table 2. The following points are noted with reference to this table and Figures 8 through 10:

(1) A difficulty was encountered in determining what effective cold regenerator mass to use for the program. The reason for this problem is that because of the low mass of the actual

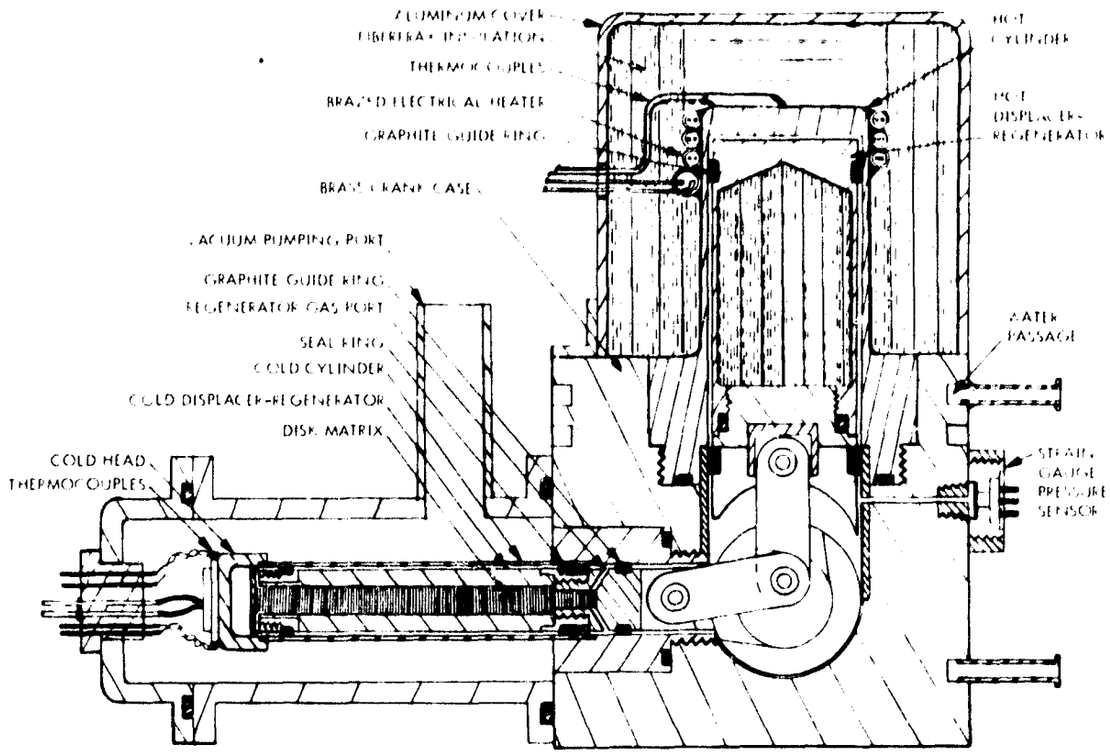

Figure 7A. RCA VM Engine, Full Size Cross-Sectional View

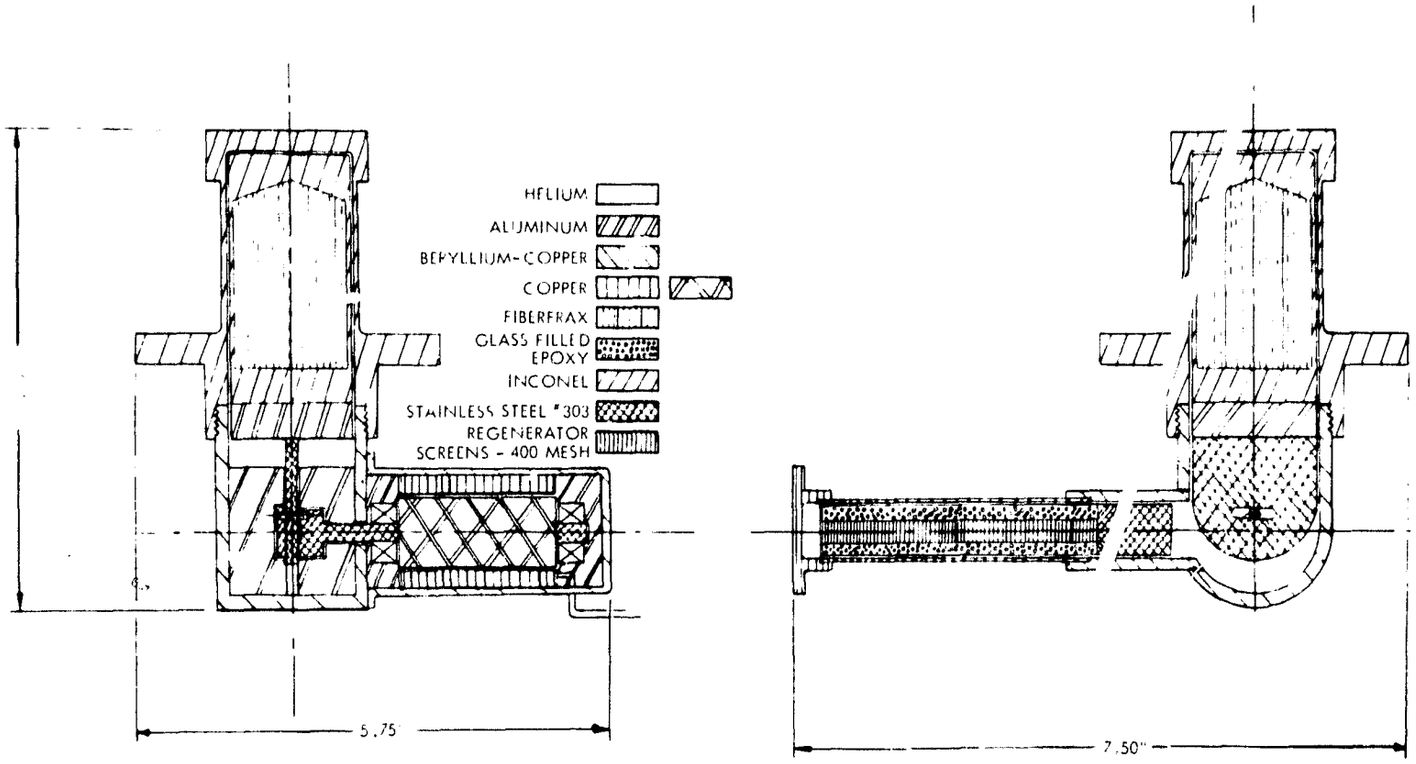

Figure 7B. Full Size, Two-View-Reference Design

Table 2

Program Results for Sample Refrigerator Design

Run No.	M_{RC}	T_{CW}	$\dot{Q}_C$	$\dot{Q}_H$	$\dot{W}K$	COP	CAR
1	.06	-320°F	1.67	140.5	5.75	.0114	.0326
2	.04	-320°F	1.11	137.7	5.7	.0076	.022
3	.0186	-320°F	- .03	134	5.55	-	-
4	.04	-357°F	-2.8	147.7	7.65	-	-
5	.04	-345°F	-1.48	142.1	6.87	-	-
6	.06	-330°F	.584	141.8	6.19	.00394	.0124

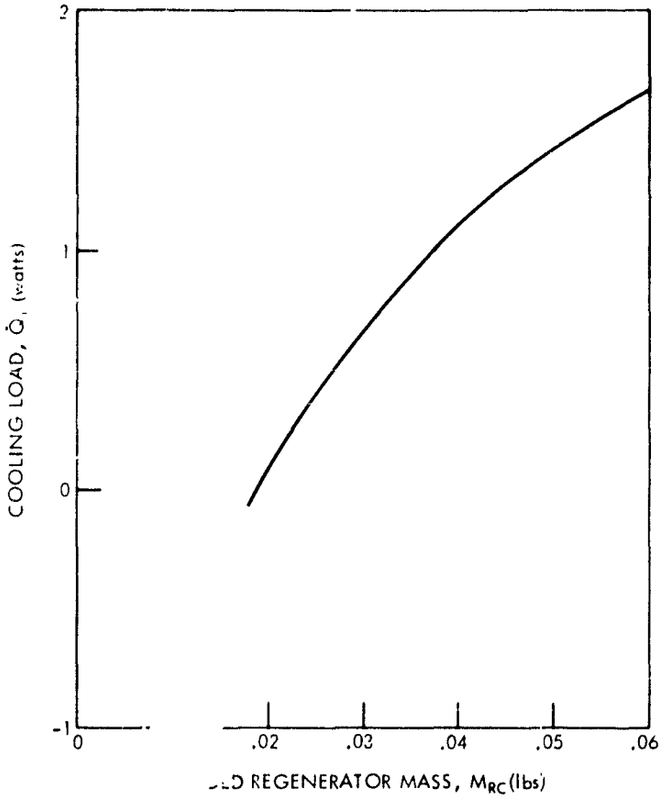

Figure 8. Cooling Load vs. Effective Cold Regenerator Mass for Sample Refrigerator. T_C = -320°F.

regenerator screening material, the obtainable cooling for a given cold cylinder temperature is sensitive to any additional regeneration which may occur at the inlet or outlet of the cold regenerators. The various possible sites for regeneration at the inlet and outlet to the regenerator were thus investigated. It was determined that the stainless steel gas port insert at the base of the cold displacer (Figure 7) provides enough effective mass and heat transfer capability for regeneration. This effective mass was calculated by computing the effective depth of penetration of a sinusoidal temperature variation in the inside and outside surfaces of the insert (Reference 5).

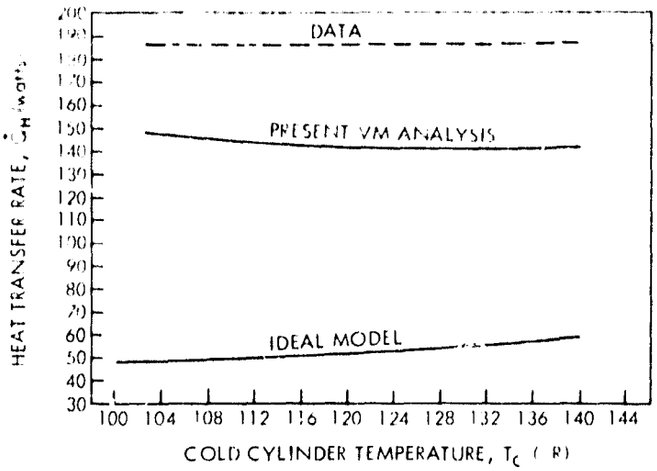

Figure 9. Hot Cylinder Power Computations for Sample Refrigerator

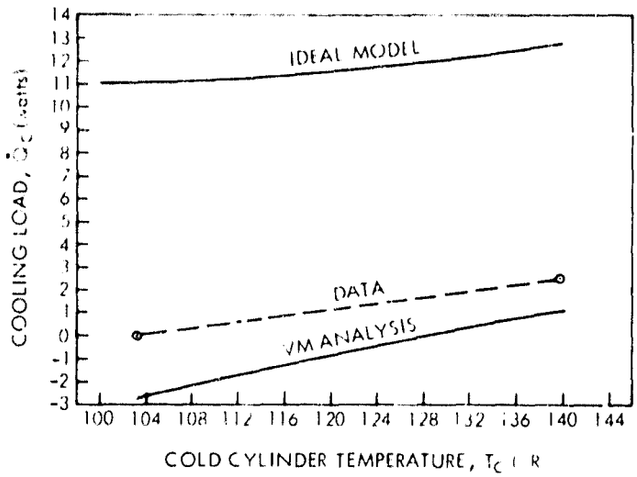

Figure 10. Cooling Load Computations for Sample Refrigerator

(2) Figure 8 shows the calculated cooling load vs. the effective cold regenerator mass for T_C = -320°F. The lowest cooling load point includes only the screens as the effective mass, while the high point includes the effective mass of the whole inside and outside surfaces of the stainless insert. The middle point also includes as the effective mass the inside surface of the stainless insert, but only half the length of the outside surface (i.e., from the gas ports to just beyond the carbon rings). It was felt that because of the influence of the outside wall which is at the ambient wall temperature, the most realistic estimate of the effective regenerator mass is .04 lbs (i.e., the middle point in Figure 8.) Therefore, the correlations between theory and data which follow use this value for the cold regenerator mass. Finally, it is of interest to note that the convex shape of the curve in Figure 8 is expected, since the greater the cold regenerator mass, the less effect a change in the mass has on the obtainable cooling load.

(3) Comparisons between the calculations and data are shown in Figures 9 and 10.

Figure 9 shows that there is very good agreement between the data and the present analysis, especially when compared to the ideal analysis. Furthermore, most of the difference between the hot cylinder heat transfer rate of the data and of the analysis can be attributed to insulation and lead wire losses which are not included in the analysis.

Figure 10 shows only two data points, with a linear interpolation between them. It is seen that the VM analysis results agree much more closely with the data than does the ideal model, especially at the higher cold-cylinder temperatures. For example, at Tc = 140°R (≈ 77K), the program predicts an obtainable cooling load of 1.1 watts, as compared to 2.5 watts measured, while the ideal model predicts 12.8 watts. At the colder cylinder temperatures the agreement between the present

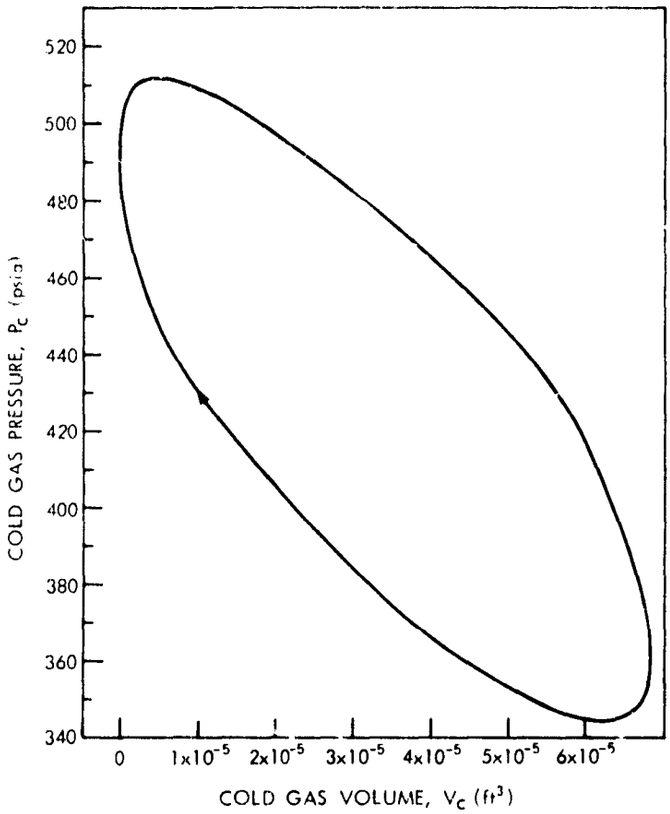

Figure 11. P_C - V_C Diagram for Sample Refrigerator

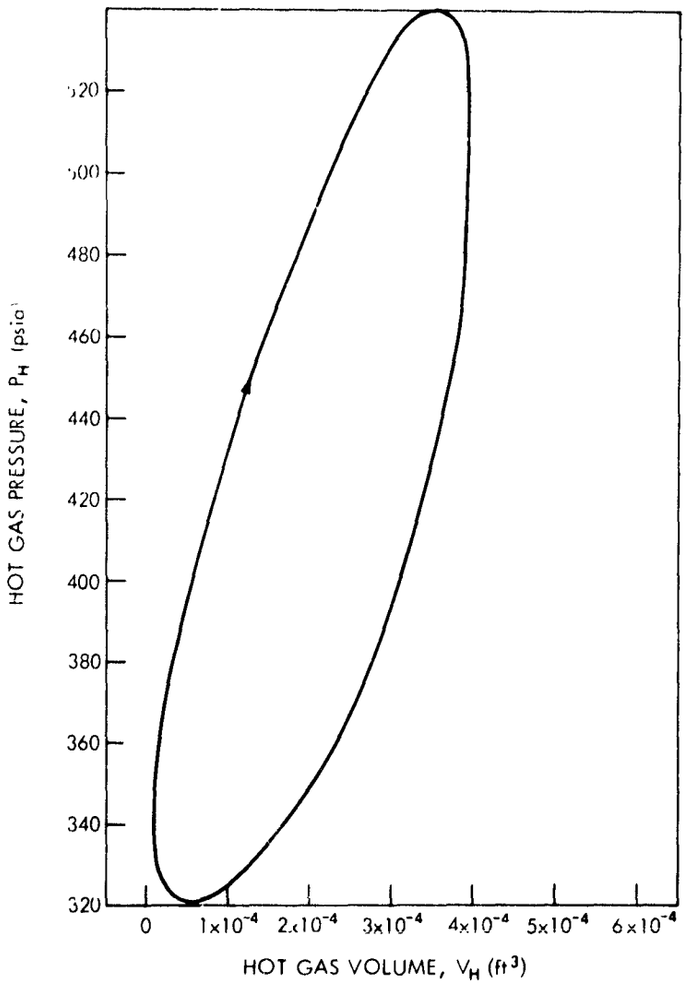

Figure 12. P_H -V_H Diagram for Sample Refrigerator

model and data is not as good, although still much closer than the ideal model. (Note that a negative cooling load means that at the corresponding cold cylinder temperature, the net heat would be transferred from the cold cylinder to the load.) The reason for the wider discrepancy at the lower cold cylinder temperatures might be the assumption of a constant matrix specific heat along the length of the cold regenerator. Obviously this assumption becomes less accurate as the difference between the temperatures at the ends of the cold regenerator increases.

(4) It is concluded that good agreement exists between the program and the available data. Furthermore, it is felt that the agreement with respect to cooling load would be even better for a refrigerator with a cold regenerator that was not quite as marginally designed (i.e., less sensitive to changes in regenerator mass). Finally, several suggestions are proposed in Section VII which should further improve the correlation for the cold end of the refrigerator.

B. Illustrative Results of Program Utility

The computed P-V diagrams for the hot and cold cylinders of the sample refrigerator are shown in Figures 11 and 12. The area enclosed by the cold-end curve divided by the period of

revolution represents the maximum possible cooling load for the refrigerator under the specified operating conditions, while the area enclosed by the hot side P-V diagram divided by the period of revolution represents the minimum possible power requirement for the refrigerator design. Hence, the feasibility of the design with respect to geometric considerations (i.e., hot cylinder size, cold cylinder size, dead volume, etc.) can be checked.

The differences between the final calculated cooling level and hot cylinder power input computed from the program, and those calculated from the P-V diagrams are due to regenerator inefficiencies, non-isothermal heat transfer from the gas to the cylinder walls, gas leakage around the displacers, and conduction losses. As an example, for the sample design $\dot{Q}_C$ and $\dot{Q}_H$ are 9.3 watts and 70.5 watts respectively from the P-V diagrams, as compared to 1.11 watts and 137.7 watts for the final calculated values. It is obvious, therefore, that there are substantial losses from the aforementioned processes.

Regenerator performance can be evaluated with the aid of Figures 13 and 14, which were composed from program data. Figure 13 shows the gas mass flow rate at the cold end of the cold regenerator as a function of crank position. The positive values are the mass flow rates of gas

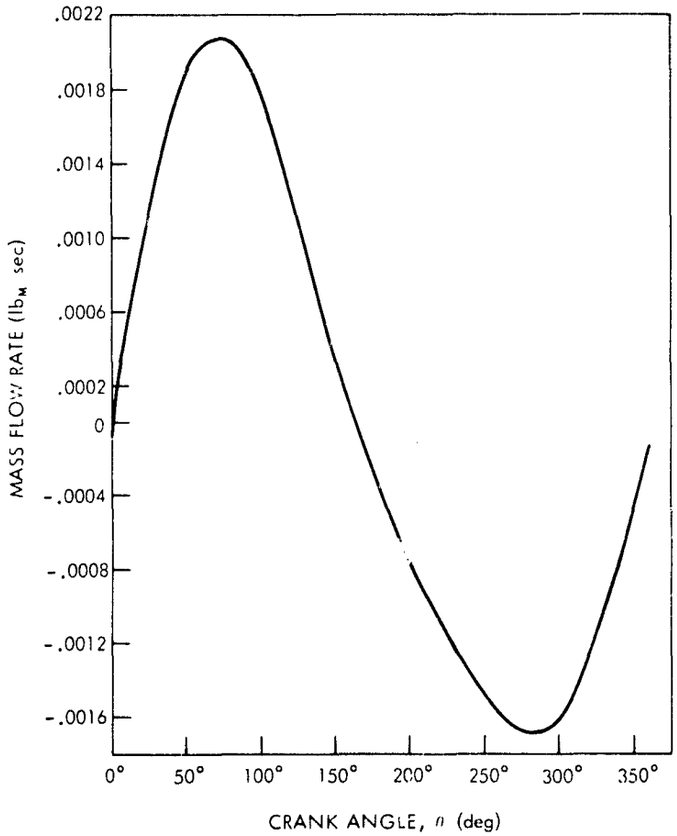

Figure 13. Mass Flow Rate of Gas at Cold End of Cold Regenerator vs. θ for Sample Regenerator.

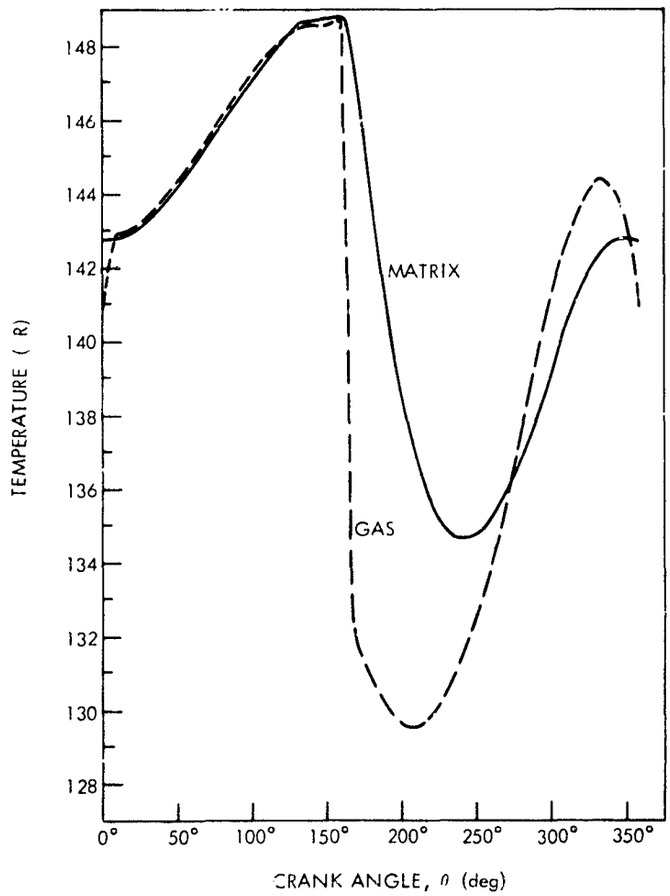

Figure 14. Matrix and Gas Temperatures of Cold of Cold Regenerator vs θ for Sample Refrigerato

leaving the regenerator and entering the cold cylinder. The negative values are the mass flow rates of gas leaving the cold cylinder and entering the cold regenerator. Figure 14 shows the matrix and gas temperatures at the extreme cold end of the cold regenerator as functions of crank angle.

During steady state operation, as the crank turns from the zero degree position the helium flows through the regenerator into the cold cylinder; hence, the mass flow rate is positive in Figure 13. The gas, as it flows through the cold regenerator, is cooled to the temperatures shown in Figure 14. At the same time the temperature of the matrix at the cold end of the cold regenerator increases as it is heated by the exiting gas. This process results in increasing the gas exit and matrix temperatures until the flow direction reverses at $\sim 165°$ (Note the minor irregularity at the peak of the curves in Figure 14, in which the gas temperature curve crosses over the matrix temperature curve, while the gas mass flow rate is still positive. This irregularity appears to be due to a minor numerical instability at the area of the peak.) As the gas mass flow rate reverses, the gas temperature is identical to the cold cylinder gas temperature. The flow of this cold gas over the regenerator's cold end lowers the matrix temperature as shown in the figure. Following this, the cold cylinder gas temperature first increases and then decreases, with a corresponding matrix temperature as shown. Finally, as the flow rate direction reverses again at $\sim 0°$, this whole process starts over again.

The regenerator's heat loss per cycle can be expressed by

$$Q_{Loss} = \int h_{1C} \dot{M}_{2C} \, dt \tag{62}$$

$$= \frac{1}{\omega} \int C_p T_{1C} \dot{M}_{2C} \, d\theta \tag{63}$$

where T_{1C} is the gas temperature shown in Figure 14 and $\dot{M}_{2C}$ is the mass flow rate shown in Figure 13. By means of Figures 13 and 14, therefore, the regenerator inefficiency can easily be calculated. Note, however, that this loss is coupled with the fluctuation of the cold cylinder gas temperature, since this fluctuation affects the temperature swing of the matrix. In this way, therefore, the program can be used to design, or to improve existing designs, of regenerators. In the present case, it is obvious (without going through the above computation) from the large matrix temperature swing that an increase in the mass of the cold regenerator would significantly increase the obtainable cooling loads. This conclusion was also reached in Section VI A.

Another regenerator design variable which can be studied with the program is the gas pressure drop across the matrix. This is particularly important in designing the seals for a refrigerator

for long life-time operation. As an example, Figure 15 shows the cold and ambient cylinder pressures vs. crank angle for the sample refrigerator, where the difference between the curves is the differential pressure across the cold displacer seals. Similar curves for the hot cylinder show a maximum pressure drop on the order of 1 psi across the hot regenerator.

Cylinder-to-gas heat transfer coefficients, gas leakage effects, and conduction losses can best be evaluated by making several computer runs for a specific refrigerator design, with several different values for the constants which represent these effects.

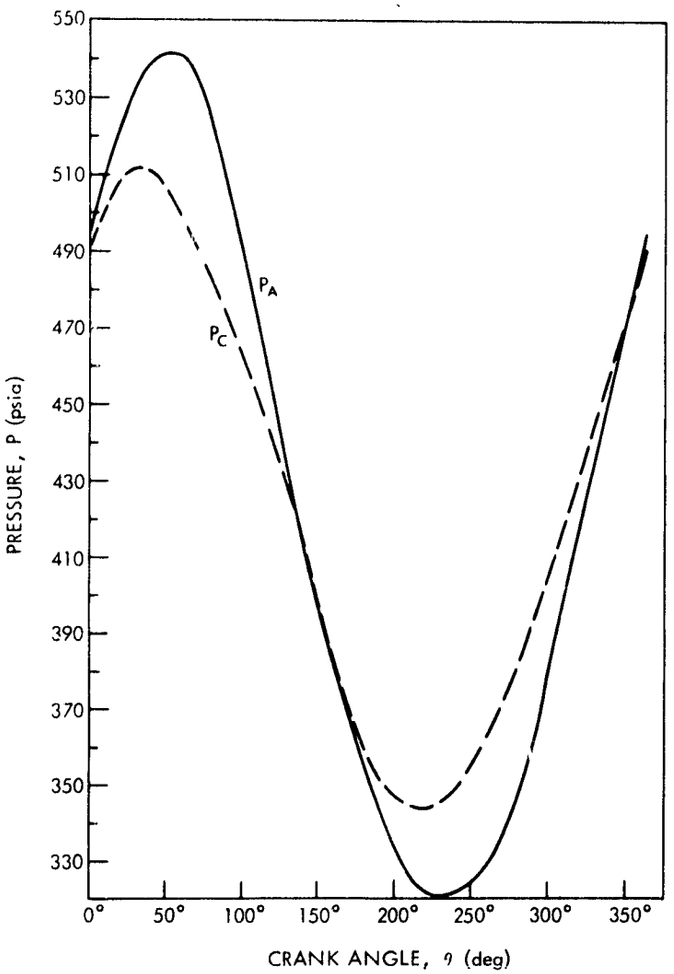

Figure 15. Ambient and Cold Cylinder Pressures vs. θ for Sample Refrigerator

VII. POSSIBLE PROGRAM IMPROVEMENTS

The VM analysis program could be improved in the following ways:

(1) The regenerator matrix specific heat could be allowed to vary with temperature according to input values or functions.

(2) Regenerators composed of sections of different material could be handled by reasonably simple program modifications.

REFERENCES

1. RCA, Advanced Technology Laboratories, "ICICLE Feasibility Study," Final Report, pp. 3-5 through 3-8. Radio Corporation of America, Camden, New Jersey, 1970.

2. Finkelstein, T., "Analysis of Practical Reversible Thermodynamic Cycles," American Society of Mechanical Engineers Paper 64-117-37, 1964.

3. Kays, W. M. and London, A., "Compact Heat Exchangers," New York: McGraw-Hill Book Company, 1964.

4. Simmons, E., "Vuilleumier Engine Modification and Support," Technical Directive 734-102, Computing and Software, Inc., NASA Goddard Space Flight Center, Greenbelt, Md., April 27, 1970.

5. Carslaw. H. and Jaeger, J., "Conduction of Heat in Solids," pp. 64-70. London: Oxford University Press, 1959.

Appendix A

List of Symbols

A_D hot or cold displacer cross-sectional area

A_{DC} cold displacer cross-sectional area

A_{DH} hot displacer cross-sectional area

A_R regenerator free flow area

A_{RCF} cold regenerator free flow area

A_{RHF} hot regenerator free flow area

b gap between displacer and cylinder

CAR % of Carnot COP

C_{KR1} cold regenerator flow resistance coefficient defined by Equation (45)

C_{KR2} cold regenerator flow resistance coefficient defined by Equation (43)

C_p gas specific heat at constant pressure

C_{PR} regenerator matrix specific heat

COP coefficient of performance

CTAIC initial gas temperature at ambient end of cold regenerator

CTCIC initial gas temperature at cold end of cold regenerator

C_v gas specific heat at constant volume

D constant defined by Equation (36)

dm infinitesimal element of gas in regenerator

dm_1 infinitesimal element of gas entering or leaving hot cylinder

dm_2 infinitesimal element of gas leaking around hot displacer between hot cylinder and ambient cylinder

E constant defined by Equation (36)

F hot or cold displacer frictional force

F_C cold displacer frictional force

F_H hot displacer frictional force

h regenerator gas enthalpy

H_{AA} ambient cylinder-to-gas convective heat transfer coefficient times heat transfer area

H_{AHE1} ambient heat exchanger #1 convective heat transfer coefficient times heat transfer area

H_{AHE2} ambient heat exchanger #2 convective heat transfer coefficient times heat transfer area

H_{CA} cold cylinder-to-gas convective heat transfer coefficient times heat transfer area

H_{CHE} cold heat exchanger convective heat transfer coefficient times heat transfer area

h_{CR} enthalpy of gas entering or leaving cold end of cold regenerator

H_{HA} hot cylinder-to-gas convective heat transfer coefficient times heat transfer area

H_{HHE} hot heat exchanger convective heat transfer coefficient times heat transfer area

H_{KR1} hot regenerator flow resistance coefficient defined by Equation (46)

H_{KR2} hot regenerator flow resistance coefficient defined by Equation (47)

h_1 enthalpy of gas entering or leaving hot cylinder

h^* convective heat transfer coefficient between regenerator matrix and gas

h^{**} defined in Table 1

HTAIC initial gas temperature for ambient end of hot regenerator

HTHIC initial gas temperature for hot end of hot regenerator

h_2 enthalpy of gas leakage entering or leaving hot cylinder via the hot displacer (Equation (16)

IREG program print command

IRUN program print command

IRUNX program print command

ITP number of iterations for program

J constant, equal to 778.16 ft-lb/BTU

K_{CA} overall thermal conductance between cold cylinder gas and ambient cylinder gas, including conduction across the cold displacer

K_{CW} thermal conductance from cold cylinder wall directly to ambient cylinder wall

K_{HA} thermal conductance between hot cylinder gas and ambient cylinder gas, including conduction across the hot displacer

K_{HW} thermal conductance from hot cylinder wall directly to ambient cylinder wall

KR_1 regenerator flow resistance coefficient defined in Figure 6

KR_2 regenerator flow resistance coefficient defined in Figure 6

ℓ cold cylinder connecting rod length

L regenerator length

L_D length of hot or cold displacer

L_{CD} length of cold displacer

L_{HD} length of hot displacer

ℓ' hot cylinder connecting rod length

M mass

$\dot{M}$ gas mass flow rate

$\dot{m}$ regenerator gas mass flow rate

p, P pressure

$\partial M_1/\partial \theta$ regenerator mass flow rate defined by Equation (39)

$\partial M_2/\partial \theta$ regenerator mass flow rate defined by Equation (40)

P_1 average hot or cold regenerator gas pressure defined by Equation (38)

P' regenerator wetted perimeter

P_2 hot or cold cylinder gas pressure

Q heat

$\dot{Q}$ heat transfer rate

r crank radius

R gas constant

R_D displacer radius

R_{CD} cold displacer radius

R_{HD} hot displacer radius

RPM crank revolutions/minute

SMC number of cold regenerator slabs

SMH number of hot regenerator slabs

t time

T temperature

T_2 hot or cold cylinder gas temperature

T_{HIN} defined in Table 1

T_{HOUT} defined in Table 1

U gas internal energy

V volume

W (defined in Table 1)

$\dot{W}K$ work rate

x coordinate along regenerator length

XDEG program print command

XVAR program convergence constant

YVAR program convergence constant

Greek Letter Symbols

α angle between hot and cold cylinder axes

$\Delta\theta$ crank angle step size

γ C_P/C_V for gas

ω rotational speed (rad/sec)

Ψ hot and cold crank displacement angle (refer to Figure 5)

$\bar{\mu}_C$ cold-to-ambient leakage average gas viscosity

$\bar{\mu}_H$ hot-to-ambient leakage average gas viscosity

$\bar{\mu}_g$ hot- or cold-to-ambient leakage average gas viscosity

ρ gas density

θ crank angle (zero position is top dead center of cold cylinder)

Subscripts

A ambient cylinder gas

A1 gas entering or leaving ambient cylinder through heat exchanger #1

A2 gas entering or leaving ambient section through heat exchanger #2

AD ambient cylinder dead volume

AW ambient wall

C cold cylinder gas

CD cold cylinder dead volume

CL leakage gas around cold cylinder

CMAXD cold displaced

CR cold regenerator dead volume

CRG cold regenerator

CW cold wall

G gas

H hot cylinder gas

HD hot cylinder dead volume

HL leakage gas flow around hot displacer

HMAXD hot displaced

HR hot regenerator dead volume

HRG hot regenerator

HW hot wall

L leakage

OC gas into or from ambient end of cold regenerator

OH gas into or from ambient end of hot regenerator

1C gas flow from or into cold end of cold regenerator

1H gas flow from or into hot end of hot regenerator

R regenerator matrix

RC cold regenerator matrix

RG applies to hot or cold regenerator dead volume or length

RH hot regenerator matrix

2C gas flow from or into cold cylinder

$2\dot{m}$ gas flow from or into hot cylinder

$\dot{m}$ total mass of gas in VM refrigerator

Superscript

$\bar{}$ average

Appendix B

Derivation of Cylinder Geometric Equations (7) through (9)

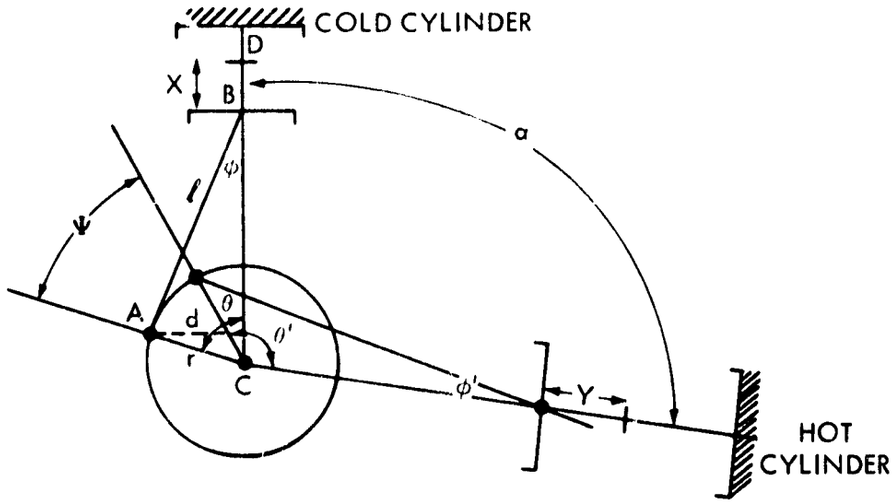

Figure B-1. Geometry of the VM Refrigerator

Referring to Figure B1,

$$x = AB + AC - DC \tag{B1}$$

$$= \ell + r - (\ell \cos \phi + r \cos \theta) \tag{B2}$$

$$= \ell (1 - \cos \theta) + r (1 - \cos \theta). \tag{B3}$$

Now

$$\frac{r}{\sin \phi} = \frac{\ell}{\sin \theta}, \tag{B4}$$

and hence

$$\sin \phi = \left(\frac{r}{\ell}\right) \sin \theta \tag{B5}$$

$$\phi = \sin^{-1} \left(\frac{r}{\ell}\right) \sin \theta. \tag{B6}$$

Combining (B3) and (B6)

$$x = \ell \left\{1 - \cos \left[\sin^{-1} \left(1 \frac{r}{\ell} \sin \theta\right)\right]\right\} + r\,(1 - \cos \theta). \tag{B 7}$$

But

$$x_{max} = 2\,r \tag{B8}$$

and

$$\frac{x}{x_{MAX}} = \frac{V}{V_{MAXD}}.$$

Hence

$$\frac{V}{V_{MAXD}} = \frac{1}{2} \frac{\ell}{r} \left(1 - \cos \left[\sin^{-1} \left(\frac{r}{\ell} \sin \theta\right)\right]\right) + \frac{1}{2} (1 - \cos \theta). \tag{B9}$$

Now, adding the dead volume to this equation, we have

$$V_C = \frac{V_{CMAXD}}{2} \left\{\frac{\ell}{r} \left(1 - \cos \left[\sin^{-1} \left(\frac{r}{\ell} \sin \theta\right)\right]\right) + (1 - \cos \theta)\right\} + V_{CD}, \tag{B10}$$

which is Equation (16)

Equation (8) can be derived in exactly the same way, but with the substitution

$$\theta' = \alpha + \theta - \Psi.$$

Equation (9) follows from a volume balance on one whole refrigerator.

Appendix C

Program Input and Output

1. Input

The program input is shown on the next two pages, which are based on material from Reference 4.

2. The program output consists of the following information:

a. Cylinder pressures as functions of θ.

b. Cylinder temperatures as functions of θ.

c. All internal gas mass flow rates as functions of θ.

d. Cylinder volumes and volumetric time rates of change as functions of θ.

e. Cold and hot regenerator gas and matrix temperatures as functions of θ.

f. Hot cylinder power requirement, cold cylinder cooling load, motor power requirement and ambient heat rejection for the input conditions.

Company COMPUTING & SOFTWARE, INC.

Application VM Input Data by E. Simmons Date 4/6/70 Job No T/D 734-102 Sheet No 1 of 2

CARD 1		VCMAXD	VHMAXD	R			RPM	VCD	DATA 1	
CARD 2		V_{AD}	V_{HD}	C_p		C_v	T_{AW}	T_{CW}	DATA 2	
CARD 3		T_{HW}	b_c	b_H	A_{nC}	A_{DH}	L_{HD}	L_{CD}	DATA 3	
CARD 4		R_{CD}	R_{HD}	L_{CRG}	L_{HRG}	P'_{CRG}	P'_{HRG}	C_{PRC}	DATA 4	
CARD 5		C_{PRH}	E_{CRG}	E_{HRG}	D_{CRG}	D_{HRG}		K_{HW}	DATA 5	
CARD 6		T_A	T_C	T_H	P_A	P_C	P_H	K_{CW}	DATA 6	

Company COMPUTING & SOFTWARE, INC.

Application VM Input Data by E. Simmons Date 4/6/70 Job No T/D 734-102 Sheet No 2 of 2

CARD 7		H_{HA}	H_{CA}	H_{AA}	K_{CA}	K_{HA}	H_{CHE}	H_{HHE}	DATA 7
CARD 8		H_{AHE1}	H_{AHE2}	C_{KR1}	H_{KR1}	H_{KR2}	C_{KR2}	M_{RC}	DATA 8
CARD 9		M_{RH}	μ_C	μ_H	A_{RCF}	A_{RHF}	V_{CR}	V_{HR}	DATA 9
CARD 10		ℓ	ℓ'	r	XDEG	XVAR	YVAR		DATA 10
CARD 11		ITR	IRUN	IRUNX	SMC	SMH	IREG		DATA 11
CARD 12		CTAIC	CTCIC	HTAIC	HTHIC				DATA 12